AIIM

Association for Information and Image Management
1100 Wayne Avenue, Suite 1100
Silver Spring, Maryland 20910
301/587-8202

Centimeter

Inches

MANUFACTURED TO AIIM STANDARDS
BY APPLIED IMAGE, INC.

1 of 1

PET Detector Modules Based on Novel Detector Technologies†

William W. Moses, Stephen E. Derenzo, and Thomas F. Budinger
Lawrence Berkeley Laboratory, University of California, Berkeley, CA 94720

ABSTRACT

A successful PET detector module must identify 511 keV photons with: high efficiency (>85%), high spatial resolution (<5 mm fwhm), low cost (<$600 / in^2), low dead time (<4 μs in^2), good timing resolution (<5 ns fwhm for conventional PET, <200 ps fwhm for time of flight), and good energy resolution (<100 keV fwhm), where these requirements are listed in decreasing order of importance. The "high efficiency" requirement also implies that the detector modules must pack together without inactive gaps. Several novel and emerging radiation detector technologies could improve the performance of PET detectors. Avalanche photodiodes, PIN photodiodes, metal channel dynode photomultiplier tubes, and new scintillators all have the potential to improve PET detectors significantly.

INTRODUCTION

Positron emission tomography (PET) is a nuclear medical imaging technique whereby the patient is injected with (or inhales) a biologically active tracer compound (*i.e.* a drug) that is labeled with a positron emitting isotope. The tracer accumulates in the patient, carrying the radioisotope with it. When the radioisotope decays, the emitted positron annihilates with an electron to form back-to-back 511 keV photons, which penetrate the patient and enter the PET detector ring. Individual positron annihilations are identified by simultaneous detection of these photons, and the parent radioisotope known to lie along the line connecting the two detected photons (known as a chord). The mathematical technique of computed tomography then uses these detected chords to reconstruct the spatial distribution of the radioisotope, and therefore the drug concentration in the patient. The time dependence of the drug uptake also contains metabolic information. This technique has been successfully applied to neurological, cardiovascular, and oncological medicine [1].

An individual PET detector module must identify the 511 keV photons exiting the patient, and for each photon detected, provide a timing pulse and a spatial location to the tomograph coincidence electronics, which then pairs detected photons based on their arrival time and assigns them to a chord based on the two interaction positions. The requirements for the detector module are, in approximate order of decreasing importance, are as follows. (1) High detection efficiency (>85% per 511 keV photon), as the chord efficiency is the square of this individual photon efficiency and PET scans are generally "starved" for statistics. This requirement also implies that the detector modules must pack together without inactive gaps. (2) High spatial resolution (<5 mm fwhm), as the detector spatial resolution is the main factor influencing the spatial resolution in the reconstructed image. (3) Low cost (parts cost <$600 / in^2 of "front" surface area), as virtually all PET cameras are commercially manufactured. (4) Low dead time (<4 μs in^2), for the high counting rates found during transmission scans and with short half-lived radioisotopes. The figure of merit given for dead time is the product of the detector dead time and the front surface area of the portion of the detector that is dead. (5) Good timing resolution (<5 ns fwhm), in order to reduce the accidental coincidence rate, which is proportional to the square of the single photon rate. If very good timing resolution is achieved (<200 ps fwhm), the arrival time difference can be used to localize the radioisotope position along the length of the chord. (6) Good energy resolution (<100 keV fwhm), in order to reject photons that have Compton scattered in the patient.

When evaluating different materials for stopping the 511 keV photons, one must consider

†This work was supported in part by the U.S. Department of Energy under contract No. DE-AC03-76SF00098, and in part by Public Health Service Grant Nos. P01 HL25840, R01 CA48002, and R01 NS29655.

both the attenuation length and the type of interactions the 511 keV photons have in the material. Photoelectric interactions are greatly preferred over Compton scatter, as a 511 keV photon that interacts via Compton scatter deposits energy in two (or more) locations in the detector ring, frequently separated by 1 cm or greater, and thus reduces the spatial resolution of the detector module. A convenient figure of merit for evaluating materials is the photoelectric attenuation length, which is the attenuation length divided by the photoelectric fraction (*i.e.* $\sigma_p / (\sigma_p+\sigma_c)$, where σ_p and σ_c are the cross sections for photoelectric effect interactions and Compton scatter interactions at 511 keV) [2]. Low values of this length are desired, as this implies both short attenuation length and high photoelectric fraction.

EXISTING DETECTOR MODULES

Current commercial PET cameras generally use detector modules similar to that shown in Figure 1 [3]. The 511 keV photons interact in the BGO (bismuth germanate, or $Bi_4Ge_3O_{12}$) scintillator crystal, and the resulting scintillation light observed by four photomultiplier tubes (PMTs). BGO is usually the scintillator of choice, as its 2.6 cm photoelectric attenuation length (1.1 cm attenuation length, 43% photoelectric fraction) is lower than any other commonly available scintillator. The 30 mm depth of the BGO crystal is nearly 3 attenuation lengths, ensuring high detection efficiency. Saw cuts in the BGO define "individual" crystal elements by controlling the light distribution among the four PMTs, and Anger logic (*i.e.* analog ratios among the four PMT signals) is used to determine which of the "individual" crystals the interaction occurred in. The sum of the four PMT signals is used to form a timing pulse (with 3 ns fwhm accuracy) and a measurement of the photon energy (with 100 keV accuracy). The size of the "individual" crystal elements determines the position resolution of the detector module, but a limited number of crystals (typically ≤64) can be accurately decoded due to the limited light output of BGO. The entire module is "dead" for approximately 1 μs after a 511 keV photon interaction while the BGO emits its scintillation light (its decay time is 300 ns), as interaction in any other portion of the module during this time would confuse the Anger logic. Assuming a price for BGO of $20 per cc and a price of $200 per PMT (independent of size), the parts cost for this detector module is $600/in^2.

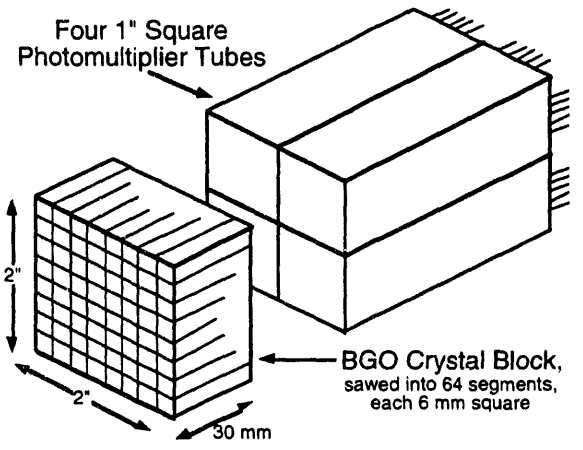

Fig. 1: "Conventional" PET Detector Module.
The "conventional" block detector module consists of a 2" x 2" x 30 mm BGO crystal that is sawed into 64 segments, each 6 mm x 6 mm x 30 mm deep. When a 511 keV photon interacts in any of the segments, the scintillation light is distributed across the back face of the BGO crystal, where it is simultaneously measured by four 1" square PMTs. The sum of the four output signals is used to derive both a timing signal and a signal proportional to the energy deposit. Anger logic (*i.e.* the ratio of the light observed in each of the four PMTs) is then used to determine the segment of interaction.

To evaluate competitive designs, we set the performance goals of improving the spatial resolution by a factor of two (*i.e.* reducing the crystal size from 6 mm square to 3 mm square) and decreasing the dead time figure of merit by a factor of four. Another important goal, albeit difficult to achieve, is to make the spatial resolution uniform over the field of view by eliminating an artifact known as radial elongation. Figure 2 shows the origin of this artifact, which is due to 511 keV photons impinging on the detector crystals at an oblique angle. Because of the 1.1 cm attenuation length of BGO, these photons can penetrate into adjacent crystals before they interact and are detected, which causes mis-positioning errors (*i.e.* events are assigned to chords that do not pass through the source). This spatial resolution degradation increases for objects placed further away from the center of the tomograph ring. If the detector module were able to measure the position (in

the radial direction) of the 511 keV photon interaction in the BGO with sufficient accuracy (5 mm fwhm), then the interactions would be assigned to the proper chord and this artifact could be eliminated [4]. No tomograph, commercial or research, yet has the ability to make this measurement, which is commonly known as depth of interaction measurement.

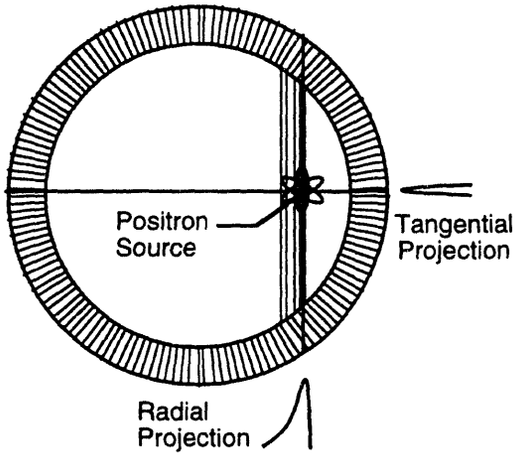

Fig. 2: Radial Elongation in PET.
511 keV photons impinging on the detector ring at an oblique angle can penetrate into adjacent crystals before they interact and are detected. This leads to mis-positioning errors that increase in severity as the source moves further away from the center of the tomograph ring. Due to the detector geometry, the radial projection (relative to the tomograph ring) is affected while the tangential projection is not affected, hence it is known as radial elongation. If the position of interaction (within the crystal) is measured with sufficient accuracy (5 mm fwhm), event pairs can be assigned to the proper chord and this artifact removed.

These design goals could be accomplished (without depth of interaction measurement) using a conventional detector module with the linear dimensions on the front surface reduced by a factor of two (*i.e.* having a 1" square by 30 mm deep BGO crystal cut into 64 3 mm square "individual" elements, read out by four 0.5" square PMTs). However, the parts cost for this detector module is $\$1200/in^2$ due to the increased number of PMTs needed to cover a square inch.

NOVEL PHOTODETECTORS

Numerous novel and emerging photodetector technologies could be incorporated into PET detectors in ways that could also meet these goals. One promising category of photodetector is devices that are small (the size of an individual 3 mm square crystal) but have sufficiently high gain bandwidth product to provide an accurate timing signal and energy measurement. Examples of such devices are multi-anode PMTs [5], metal channel dynode PMTs [6], avalanche photodiode (APD) arrays [7], segmented vacuum avalanche phototubes [8], and VLPCs (visible light photon counters) [9]. These devices would be incorporated into a PET detector module as shown in Figure 3. The individual crystals are now decoupled, both optically and electronically, and so the position of the crystal of interaction is determined merely by identifying the photodetector that fires. The depth of interaction is measured by coating the crystals with a "lossy" reflector, so the ratio of the light observed in the "front" photodetector (*i.e.* the one closest to the patient) and the "back" photodetector depends on the position of the 511 keV photon interaction.

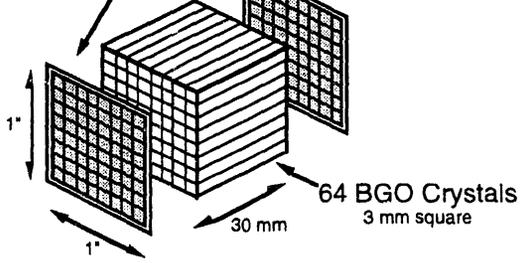

Fig. 3: High Gain-Bandwidth Photodetector Module.
With high gain-bandwidth photodetectors, a module would consist of 64 optically isolated BGO crystals, each 3 mm x 3 mm x 30 mm deep and coated with a "lossy" reflector. When a 511 keV photon interacts in any of the elements, the scintillation light is detected by photodetectors at either end of the crystal. The sum of the two output signals is used to derive a timing signal and a signal proportional to the energy deposit, and the ratio used to determine the depth of interaction.

While this type of detector module has the desired spatial resolution improvement due to the smaller (3 mm square) crystals, its main advantage is that the crystals are completely decoupled, and so a much smaller area is inactivated for the 1 μs that the BGO is emitting light. This

decreases the dead time figure of merit by the ratio of the conventional block detector front surface area to the individual crystal front surface area, a factor of 256 in our proposed geometry.

However, many of the novel photodetectors mentioned as possibilities have severe drawbacks. Some, such as multi-anode PMTs, segmented vacuum avalanche phototubes and possibly metal channel dynode PMTs, have a large dead area surrounding the photosensitive area, which would make them difficult to incorporate into PET detector modules that can be packed together without gaps. The VLPC must operate at cryogenic temperatures (6–8 K), which makes coupling the scintillator to the photodetector difficult. While light guides or fiber optics might solve either of these problems, they significantly reduce the amount of light at the photodetector, impairing the timing and energy resolution. Finally, cost is a major consideration, as the cost per unit area of these photodetectors must be about $\$100/in^2$ (half that of a conventional PMT) or about $\$200/in^2$ if the ability to measure depth of interaction is eliminated. Thus, we feel that metal channel dynode PMTs (if they can be manufactured with low dead area around their periphery) and avalanche photodiode arrays are the most promising photodetectors in this category, largely due to their potential to be inexpensive.

There is another class of new and emerging photodetectors that do not have sufficient gain bandwidth product to generate an accurate timing signal. Examples of these are PIN photodiode arrays, silicon drift photodiode arrays [10], and high band-gap photodetectors (such as HgI_2 [11], TlBr(I) [12], and InI [13]). These devices could be incorporated into a PET detector module that meets the design goals by assembling a module as shown in Figure 4. The PMT provides an accurate timing pulse whenever a 511 keV photon interacts in any of the individual crystals, and the photodetector array determines which crystal the interaction occurred in. If the photodetectors have sufficient signal to noise ratio, the reflector around the crystals can be "lossy" and the ratio of the PMT and photodetector pulse heights used to measure the depth of interaction [14].

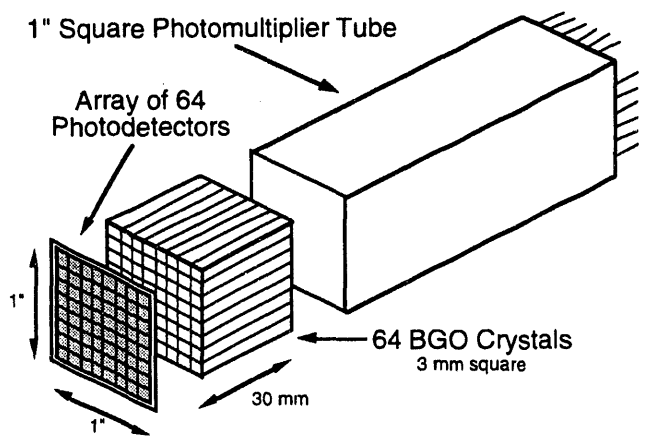

Fig. 4: Low Gain-Bandwidth Photodetector Module.
With low gain-bandwidth photodetectors, a module would again consist of 64 optically isolated BGO crystals, each 3 mm x 3 mm x 30 mm deep and coated with a "lossy" reflector. When a 511 keV photon interacts in any of the elements, the scintillation light is detected by a PMT at one end of the crystal and the photodetector array at either end of the crystal. The PMT output is used to derive a timing signal and a signal proportional to the energy deposit, and the PMT / photodetector ratio used to determine the depth of interaction.

A PET detector module of this design has the desired improvement in spatial resolution due to the 3 mm square crystals, and also improves the dead time figure of merit. This improvement is a factor of four over the conventional module (rather than the factor of 256 gained with the previous module) because all crystals connected to the PMT are dead for 1 μs when a 511 keV photon interacts in any of them. In order for this design to be practical, the photodetector array must be extremely inexpensive – significantly less than the $200 price of the PMT. Signal to noise ratio is particularly important too, as these are unity gain devices reading out very small (<1000 electron) signals. Of the technologies mentioned, the silicon based photodetectors appear to be the most promising, as they are farther developed and the equipment for fabricating them (*i.e.* silicon foundries) is more readily available.

A common misconception is that photodetectors with low timing jitter, such as microchannel plate PMTs and vacuum avalanche phototubes, would improve the timing resolution of a PET detector module. The timing resolution is actually determined by the rate at which scintillation light exits the BGO crystal. If the photodetector has a 20% quantum efficiency for the 480 nm scintilla-

tion light from BGO (a typical quantum efficiency for a PMT), it will produce approximately 250 photoelectrons per 511 keV energy deposit in the scintillator crystal. These are emitted with a 300 ns decay time, so the instantaneous photoelectron rate immediately following an interaction is 0.8 photoelectrons per nanosecond. Thus, the random fluctuations in photoelectron arrival time are significantly larger than the time jitter associated with many conventional PMTs, so no improvement in timing accuracy is expected even with a photodetector with no timing jitter.

WIRE CHAMBERS

PET detector modules can also be built from gamma converters read out by multi-wire proportional chambers, as shown in Figure 5. Examples of such gamma converters are BaF_2 / TMAE [15] and heavy metal (Pb or W) foils [16]. These detectors offer a significant reduction in cost, as wire chambers are significantly less expensive per unit area than PMTs. However, these gamma converters have significantly lower efficiency for detecting individual 511 keV gammas than BGO based systems (10%–30% as opposed to 90%), so the coincident event detection efficiency (the square of the single gamma efficiency) is severely reduced. They also produce a low number of photoelectrons per 511 keV interaction (1–5), so their energy resolution is very poor. Finally, they each are deficient in at least one other performance category – the BaF_2 / TMAE system has limited spatial resolution (5–11 mm fwhm) while the foil converters have poor timing resolution (88 ns).

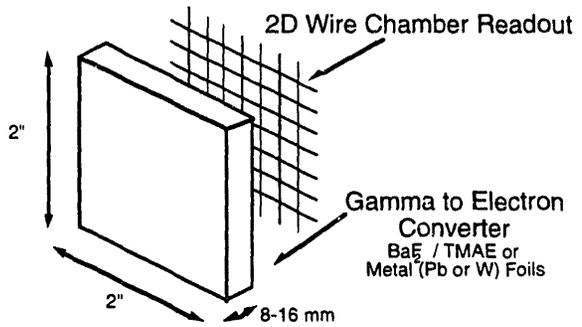

Fig. 5: Gamma Converter / Wire Chamber Readout Module.
The 511 keV photon is converted into a small number of photoelectrons either by a heavy metal foil (Pb or W) or by a BaF_2 scintillator / TMAE gas combination. These electrons are collected by a multi-wire proportional chamber, which generates a timing pulse and identifies the interaction position.

ACTIVE GAMMA DETECTORS

Advances have also been made in "active" gamma detectors (*i.e.* devices that directly convert the incident gamma into an electrical signal), both solid state detectors (such as CdTe [17], CdZnTe [18], PbI_2 [19], HgI_2 [11], high purity germanium, and silicon) and liquid proportional chambers (such as liquid xenon [20]), and PET detector modules (such as in Figure 6) could be made with these elements in place of the BGO scintillator. While their main advantage is their energy resolution, which is as good as 2 keV fwhm, they tend to encounter problems due to the low drift velocities (10^3–10^5 m/s) of the electrons and holes. The detectors must be approximately 3 radiation lengths thick in order to have sufficient efficiency for detecting 511 keV photons, which translates to detector thicknesses of at least 10 cm and charge collection times of hundreds of microseconds. This makes coincidence timing unacceptably long (except for liquid xenon, in which prompt scintillation light can be used to create a timing pulse) and causes event pileup in the detector volume at comparatively low rates (single event rates in PET approach 10^6 events/sec/in^2, and higher rate capability is desired). These problems could be reduced, but not eliminated, by using more complicated collection electrode schemes than the simple one described here.

These devices also suffer a performance drawback in that their low atomic number gives them a long photoelectric attenuation length compared to BGO (3.6 cm for PbI_2, 3.7 cm for HgI_2, 11 cm for CdTe and CdZnTe, 16 cm for liquid xenon, 55 cm for germanium, and 2400 cm for silicon, as opposed to 2.6 cm for BGO), so their spatial resolution is also degraded. Finally, both solid state and liquid proportional chambers have additional practical disadvantages. Very few solid state detectors can currently be grown in the large sizes required for PET, and it is

not clear that the required volumes could ever be produced inexpensively. Liquid proportional chambers require refrigeration to approximately −100° C, and geometrical constraints are imposed if proportional mode (with gain, as opposed to unity gain ion chamber mode) of wire chamber operation is desired, as proportional gain can only be achieved in the gas phase and so a gas / liquid interface must be maintained.

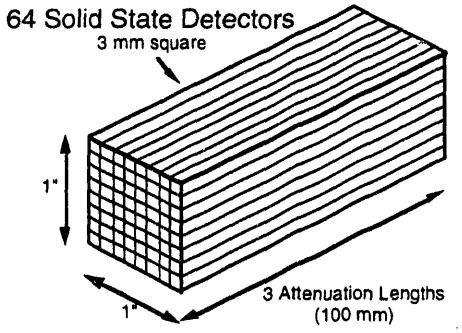

Fig. 6: Active Gamma Detector Module. The 511 keV photon is converted in the "active" detector into a large number of electron hole pairs. These electrons drift with relatively slow velocity to the end of the detector, where they are collected to identify the position of interaction and generate a timing pulse. If the active detector is liquid xenon, a timing pulse can be generated from the prompt flash of scintillation light.

NOVEL SCINTILLATORS

Finally, advances have also been made in scintillator technology. Using the BGO as a standard, the requirements for a scintillator for PET (all quantities assume 511 keV photon energy), listed in approximate order of importance, are as follows. (1) Short attenuation length (<1.1 cm). This affects the ability of the scintillator to stop the annihilation photons, and thus the spatial resolution. (2) High photoelectric fraction (>43%). This affects the fraction of events that yield a single, well positioned energy deposit in the detector module, and thus the spatial resolution. (3) Low photoelectric attenuation length (<2.6 cm). This is just the attenuation length divided by the photoelectric fraction, and so is a convenient single metric for evaluating the capability of the scintillator for high spatial resolution. (4) Short scintillation decay time (<300 ns). This reduces the dead time and improves the coincidence timing accuracy. This is probably the largest deficiency of BGO for PET. (5) Cost (<$20/cc). (6) High light output. This affects the energy resolution, the spatial resolution (more light means that a conventional detector module using Anger logic can decode more, and thus smaller, "individual" crystals), and the coincidence timing resolution (even with the same decay time, the instantaneous photon rate is increased).

While no readily available scintillator has superior properties to BGO for PET, there has been a resurgence of work in scintillator development in the past few years and some very promising compounds developed. Since it is very unusual for a new scintillator to be different from previous scintillators in only one of the aforementioned six criteria, evaluating a new material generally entails a complex set of tradeoffs, which are best measured by how they affect the module performance requirements listed in the Introduction. The most promising new scintillator currently is LSO (lutetium orthosilicate or Lu_2SiO_5), which boasts an attenuation length of 1.2 cm, a photoelectric fraction of 34%, a decay time of 40 ns, and a light output of 25,000 photons per MeV [21]. The raw material and crystal growth costs of this material are currently quite high, but should these costs come down, the great improvement in decay time and light output will probably compensate for the reduced photoelectric fraction.

CONCLUSION

Recent advances in detector technology allow a large number of potential designs for PET detector modules. While many of these potential designs have disadvantages that discourage their use for PET, several high gain-bandwidth photodetector technologies (avalanche photodiode arrays and metal channel dynode PMTs) and low gain-bandwidth photodetector technologies (PIN and silicon drift photodiode arrays) show great potential for improving the performance of PET detectors. Improvements in scintillator materials seem very feasible and also have tremendous potential for improving PET detector performance, but it is difficult to predict in what way the improve-

ments will manifest themselves. However, the cost of any of these advanced technologies must be carefully considered, as any improvement in performance must be substantial in order to warrant an increase in cost.

ACKNOWLEDGMENTS

We thank our colleagues working in radiation detection and medical imaging research for the innumerable thought provoking discussions that have lead to this summary. This work was supported in part by the Director, Office of Energy Research, Office of Health and Environmental Research, Medical Applications and Biophysical Research Division of the U.S. Department of Energy under contract No. DE-AC03-76SF00098, and in part by Public Health Service Grant Nos. P01 HL25840, R01 CA48002, and R01 NS29655, awarded by the National Heart Lung and Blood, National Cancer, and Neurological Science Institutes, Department of Health and Human Services.

REFERENCES

[1] Special Issue on Clinical PET. *J. Nucl. Med.* **32:** pp. 561–748, 1991.

[2] Derenzo SE, Moses WW, Huesman RH, et al. Critical instrumentation issues for <2 mm resolution, high sensitivity brain PET. In Quantification of Brain Function: Tracer Kinetics and Image Analysis in Brain PET, pp. 25–37, (Edited by K. Uemura, N. A. Lassen, T. Jones and I. Kanno), Elsevier Science Publishers, Amsterdam, 1993.

[3] Tornai MP, Germano G and Hoffman EJ. Positioning and energy response of PET block detectors with different light sharing schemes. *IEEE Trans. Nucl. Sci.* **NS-41:** (Accepted for publication. Preprint in 1993 IEEE NSS Conference Record, pp. 1126–1130), 1994.

[4] Moses WW, Huesman RH and Derenzo SE. A new algorithm for using depth-of-interaction measurement information in PET data acquisition. *J. Nucl. Med.* **32:** pp. 995, 1991.

[5] Suzuki S, Nakaya T, Suzuki A, et al. PMTs of superior time resolution, wide dynamic range, and low cross-talk multi-anode PMTs. *IEEE Trans. Nucl. Sci.* **NS-40:** pp. 431–433, 1993.

[6] Kyushima H, Hasegawa Y, Atsumi A, et al. Photomultiplier tube of new dynode configuration. *IEEE Trans. Nucl. Sci.* **NS-41:** (Accepted for publication. Preprint in 1993 IEEE NSS Conference Record, pp. 709–713), 1994.

[7] Gramsch E, Szawlowski M, Zhang S, et al. Fast, high density avalanche photodiode arrays. *IEEE Trans. Nucl. Sci.* **NS-41:** (Accepted for publication. Preprint in 1993 IEEE NSS Conference Record, pp. 457–461), 1994.

[8] Cushman P and Rusack R. A photomultiplier tube incorporating an avalanche photodiode. *Nucl. Instr. Meth.* **A-333:** pp. 381–390, 1993.

[9] Kwait P, Steinberg A, Chiao R, et al. High-efficiency single-photon detectors. *Phys. Rev.* **A-48:** pp. R867–R870, 1993.

[10] Avset BS, Ellison J, Evensen L, et al. Silicon drift photodiodes. *Nucl. Instr. Meth.* **A-288:** pp. 131–136, 1990.

[11] Iwanczyk J, Dorri N, Wang M, et al. 20-Element HgI_2 energy dispersive x-ray array detector system. *IEEE Trans. Nucl. Sci.* pp. 1275–1280, 1992.

[12] Olschner F, Shah K, Lund J, et al. Thallium bromide semiconductor x-ray and gamma-ray detectors. *Nucl. Instr. Meth.* **A-322:** pp. 504–508, 1992.

[13] Squillante M, Zhou C, Zhang J, et al. InI nuclear radiation detectors. *IEEE Trans. Nucl. Sci.* **NS-40:** pp. 364–366, 1993.

[14] Moses WW and Derenzo SE. Design studies for a PET detector module using a PIN photodiode to measure depth of interaction. *IEEE Trans. Nucl. Sci.* **NS–41:** (accepted for publication), 1994.

[15] Wells K, Visvikis D, Ott RJ, et al. Performance of a BaF_2-TMAE detector for use in PET. *IEEE Trans. Nucl. Sci.* **NS-41:** (Accepted for publication.), 1994.

[16] McKee BTA, Dickson AW and Howse DC. Performance of QPET, a high-resolution 3D PET imaging system for high volumes. *IEEE Trans. Med. Img.* **MI-13:** pp. 176–185, 1994.

[17] Glasser F, Thomas G, Cuzin M, et al. Application of cadmium telluride detectors to high energy computed tomography. *Nucl. Instr. Meth.* **A-322:** pp. 619–622, 1992.

[18] Butler JF, Lingren CL and Doty FP. $Cd_{1-x}Zn_xTe$ gamma ray detectors. *IEEE Trans. Nucl. Sci.* **NS-39:** pp. 605–609, 1992.

[19] Lund J, Shah K, Olschner F, et al. Recent progress in lead iodide x-ray spectrometer development. *Nucl. Instr. Meth.* **A-322:** pp. 464–466, 1992.

[20] Chepel VY. A new liquid xenon scintillation detector for positron emission tomography. *Nucl. Trks. Rad. Meas.* **21:** pp. 47–51, 1993.

[21] Melcher CL and Schweitzer JS. Cerium-doped lutetium orthosilicate: a fast, efficient new scintillator. *IEEE Trans. Nucl. Sci.* **NS-39:** pp. 502–505, 1992.

DATE
FILMED
11/2/94

END